Preliminary draft

28 July 2022

elisa.elena.jacquet@cern.ch

Phase Methods for Precision Measurements at BASE

Elisa Jacquet
CERN, CH-1211 Geneva, Switzerland

CERN Summer Student Program 2022

Contents

1 Introduction

1.1 Overview of The BASE Experiment

The Baryon Antibaryon Symmetry Experiment (BASE) is a high-precision experiment that aims to test CPT invariance by comparing the fundamental properties of matter/antimatter conjugates with high precision. At its core is a Penning trap system used to measure and compare the charge-to-mass ratios and g-factors of protons and antiprotons [1, 2].

The charge-to-mass ratios can be inferred from the cyclotron motion of a single-trapped (anti)proton in a Penning trap with magnetic field B_0 according to [1, 2]:

$$\nu_c = \frac{qB_0}{2\pi m} \tag{1}$$

where ν_c is the particle's cyclotron frequency.

In g-factor measurements the ratio of the spin precession (or Larmor frequency ν_L) and the cyclotron frequency is measured, to obtain the g-factor according to

$$\frac{g}{2} = \frac{\nu_L}{\nu_c}. \tag{2}$$

A high-precision measurement of ν_c is therefore crucial to the measurement of both g and q/m.

In a Penning trap the free cyclotron frequency is obtained by measuring the modified cyclotron, magnetron and axial motions of the particle and applying the invariance theorem [1, 2, 3]:

$$\nu_c^2 = \nu_+^2 + \nu_-^2 + \nu_z^2, \tag{3}$$

where ν_+, ν_-, and ν_z are the particle's modified cyclotron, magnetron and axial frequencies respectively. These motions are illustrated in figure 1 (b).

The Penning traps used in BASE are 5-electrode traps that contain both a magnetic field $B = B_0\mathbf{e}_z$ and a quadrupole electric potential [1]:

$$V(\rho, z) = V_R C_2 (z^2 - \frac{\rho^2}{2}). \tag{4}$$

Here C_2 is a trap specific geometric coefficient. The magnetic field constrains the particle in its radial motion and the electric field controls the particle's motion in the $\pm z$ direction. The BASE Penning trap has 5 electrodes (as shown in figure 1 (a)). The potential difference V_R in equation 4 is the potential difference between the ring electrode and the two endcap electrodes. The two correction electrodes are tuned to eliminate higher-order perturbation terms in the expansion of $V(0, z)$ to limit these effects on the frequency of the particle. Furthermore, the (anti)particle in the trap is cooled to allow for high-precision measurements of ν_c while neglecting frequency shifts due to high-order potential terms [1, 3].

1.1.1 Phase Methods in BASE

In Penning trap experiments, phase sensitive methods have allowed for some of the most precise measurements of cyclotron frequencies [3]. The phase sensitive measurement of the

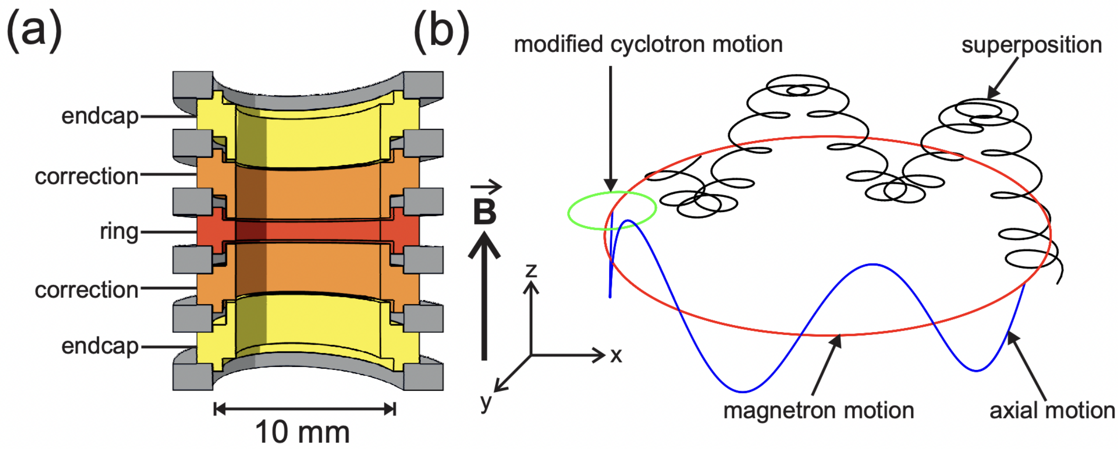

Figure 1: (a) Shows an illustration of the 5-electrode Penning trap used by the BASE experiment. (b) Shows an illustration of the three (cyclotron, magnetron and axial) motions that a trapped (anti)proton undergo inside the trap. Taken from [1]

cyclotron frequency can be achieved by either the ‘Pulse and Probe’ PnP method or the ‘Pulse and Amplify’ PnA method.

Phase methods rely on measuring the relative change in the particle’s phase to then infer its cyclotron frequency. In order to do this, the particle’s cyclotron mode is resonantly excited by an RF pulse with a well defined phase $\phi_{c,0}$. Some time t after this happens, the particle’s cyclotron phase ϕ_c will have evolved to

$$\phi_c(t) = \phi_{c,0} + \omega_+ \cdot t. \tag{5}$$

Therefore, by measuring $\phi_c(t)$, ω_+ can de determined. In practice, the phase $\phi_c(t)$ is not measured directly. Instead, the cyclotron and axial motions of the particle are coupled using an RF pulse chosen so that the axial motion takes on a phase equal to $\phi_c(t) + \phi_1$, where ϕ_1 is constant. The axial phase is then measured.

It can be shown that the RF pulse that will couple axial and cyclotron frequencies in a phase-conserving manner has frequency ω_{rf}

$$\omega_{rf} = \omega_+ \mp \omega_z + \delta \tag{6}$$

where δ is a small detuning factor. The lower frequency is used for the PnP method, and the higher one used for the PnA method. Details of the calculation can be found in Ref. [3]. The resulting equations of motion for the axial ($z(t)$) and radial ($x(t)$) are shown here.

For the PnP method, assuming that the coupling is turned on for $t_{evolution} = \pi/\Omega$ where Ω is the resonant Rabi frequency and a particle initially in the state

$$z(0) = x_0 \sin(\phi_Z) \tag{7}$$
$$x(0) = z_0 \sin(\phi_C), \tag{8}$$

we get:

$$z(t) = x_0\sqrt{\frac{\omega_+}{\omega_z}}\sin\left(\phi_C + \omega_z t\right) \tag{9}$$

$$x(t) = z_0\sqrt{\frac{\omega_z}{\omega_+}}\sin\left(\phi_Z + \omega_+ t\right). \tag{10}$$

Therefore, the coupling pulse maps the cyclotron phase onto the axial mode.

In the PnA method, the equations of motion for the same initial stated and a general coupling time t are:

$$z(t) = \frac{1}{\sqrt{\pi m\omega_z}}\left[Z_0\cosh\left(\Omega t/2\right)\cos\left(\omega_z t + \phi_z\right) + C_0\sinh\left(\Omega t/2\right)\sin\left(\omega_z t - \phi_c\right)\right] \tag{11}$$

$$x(t) = \frac{1}{\sqrt{\pi m\omega_+}}\left[C_0\cosh\left(\Omega t/2\right)\cos\left(\omega_+ t + \phi_c\right) + Z_0\sinh\left(\Omega t/2\right)\sin\left(\omega_+ t - \phi_z\right)\right]. \tag{12}$$

In this case, as the coupling time t increases, the amplitude of the axial and radial motions increase hyperbolically. In order to have a dominant phase component that comes from the cyclotron phase ϕ_c, it is necessary to excite the cyclotron motion before coupling so that C_0 dominates Z_0.

1.2 Project Overview

My project was to build a box that neatly and efficiently allows us to perform the PnP or PnA methods. The goal is to have a box that can solely control the RF pulses that are required to couple the axial and cyclotron motions, providing a centralised control for all phase methods.

The box controls the transmission of RF pulses that can cool the cyclotron motion, excite the cyclotron motion and couple the cyclotron and axial motions. It is designed such that the transmission of RF pulses are determined by either a series of TTL inputs, a user via an Arduino/LABVIEW interface, or manually through switches on the box's front panel. The box is described in greater detail in the following section of the report. The tests performed on the box are also described below.

2 Phase Methods Fast Switch Box (PM-BOX)

The goal of the phase methods fast switch box (PM-BOX) is to allow precise phase-sensitive measurements of the modified cyclotron frequency of the trapped particle. The box provides the hardware necessary to perform the 'Pulse and Probe' or 'Pulse and Amplify' phase methods. In both methods, the particle is first cooled and then, after some time, an RF signal couples the axial and modified cyclotron frequencies of the particle. Comparisons of the initial and final axial signals give the phase information.

2.1 Technical Information

2.1.1 Front Panel

The PM-BOX manages the three steps described above. The switches on the front panel allow the cooling, excitation and coupling portions of the procedure to be controlled by TTL inputs or by a user via the Arduino LabVIEW interface.
On the front of the box are 6 inputs:

- RF 1, 2, 3:
  The 3 different RF inputs that cool the particle (RF1), send the excitation pulse to the particle (RF2), and couple axial and cyclotron frequencies (RF3).

- TTL 1, 2, 3:
  These are each used to control remotely which signal (RF 1, 2, 3) goes through the box.

If more than one signal is turned on, then the box will mix them together to form the output via a signal combiner. The three switches above each input control whether that input is ON, OFF or REMOTE. In REMOTE mode, the input signal is controlled by either the Arduino or the TTL.

The front of the box also has a USB port which connects to the Arduino UNO. The switch here allows the Arduino to be reset.

Three LED lights on the front of the box show that the power supply is functioning properly.

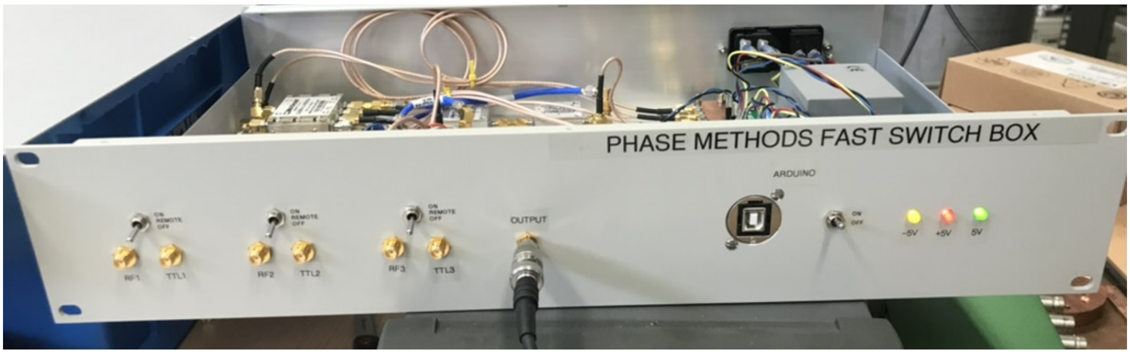

Figure 2: The front panel of the box.

2.1.2 Overview of the Box

Figure 3 shows the layout of the inside of the box. The main components are:

- LASCAR PSU-206 (Ref. [4]) Power Supply
- Power Distribution Board
- 4 Fast RF Switches (Ref. [5])
- 2 RF Combiners (Ref. [6])
- Arduino Uno
- Logic Board

The box is powered by a LASCAR PSU-206 Power Supply(Ref. [4]), whose power is redistributed to all other components in the box via the Power Distribution Board. This board has four +5V outputs and four -5V outputs, each that feeds into one of four Fast RF Switches. The Power Distribution Board also distributes 5V to the ArduinoUNO and to the Logic Board via P3 (see figure 8).

The TTL input signals and Arduino signals go through the Logic Board, controlling whether the RF Switches are in the Open or Closed position. The RF inputs each go into one of the RF Switches. The output of each RF Switch is then combined into a Master Switch. The Outut of this Master Switch is the main output of the box. Figure 4 shows a schematic of the box circuit.

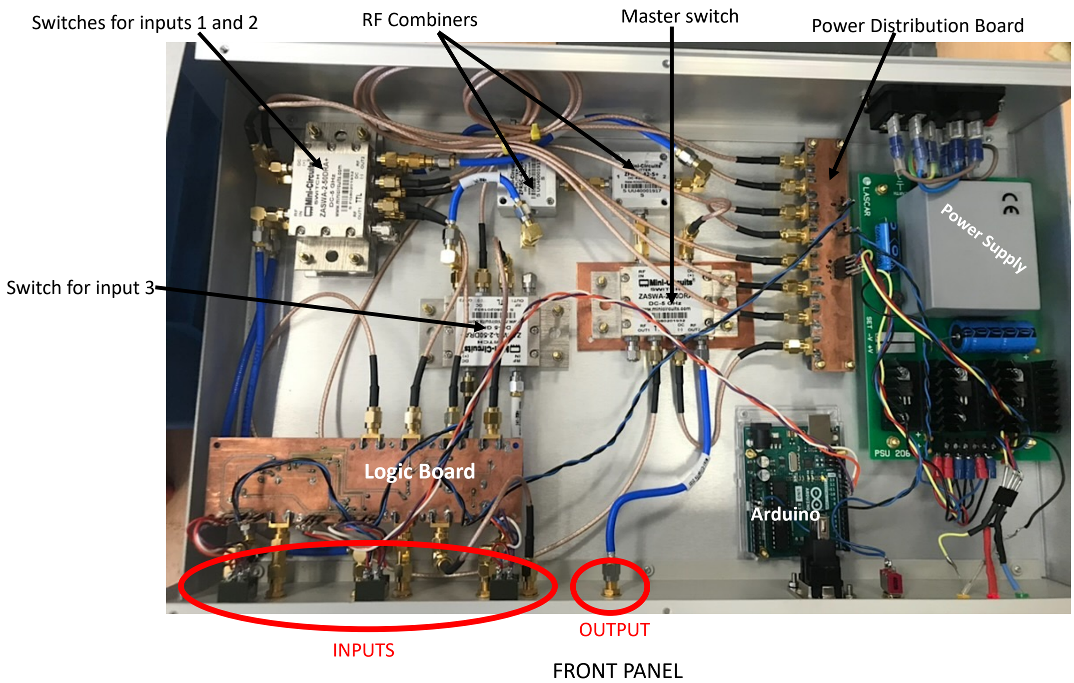

Figure 3: Layout of the box

Note on the wiring in the box:

The wires in the box are consistently kept the same colour. -5V lines are connected with yellow wires. +5V lines are connected with red wires. The 5V to power the logic board and ArduinoUNO are blue wires. Ground uses black wires.

- For the switches: white wires are used for ON, purple for OFF, and orange for REMOTE.
- For the arduino: purple goes to Input1, orange goes to Input2 and white goes to Input3 in the logic board.

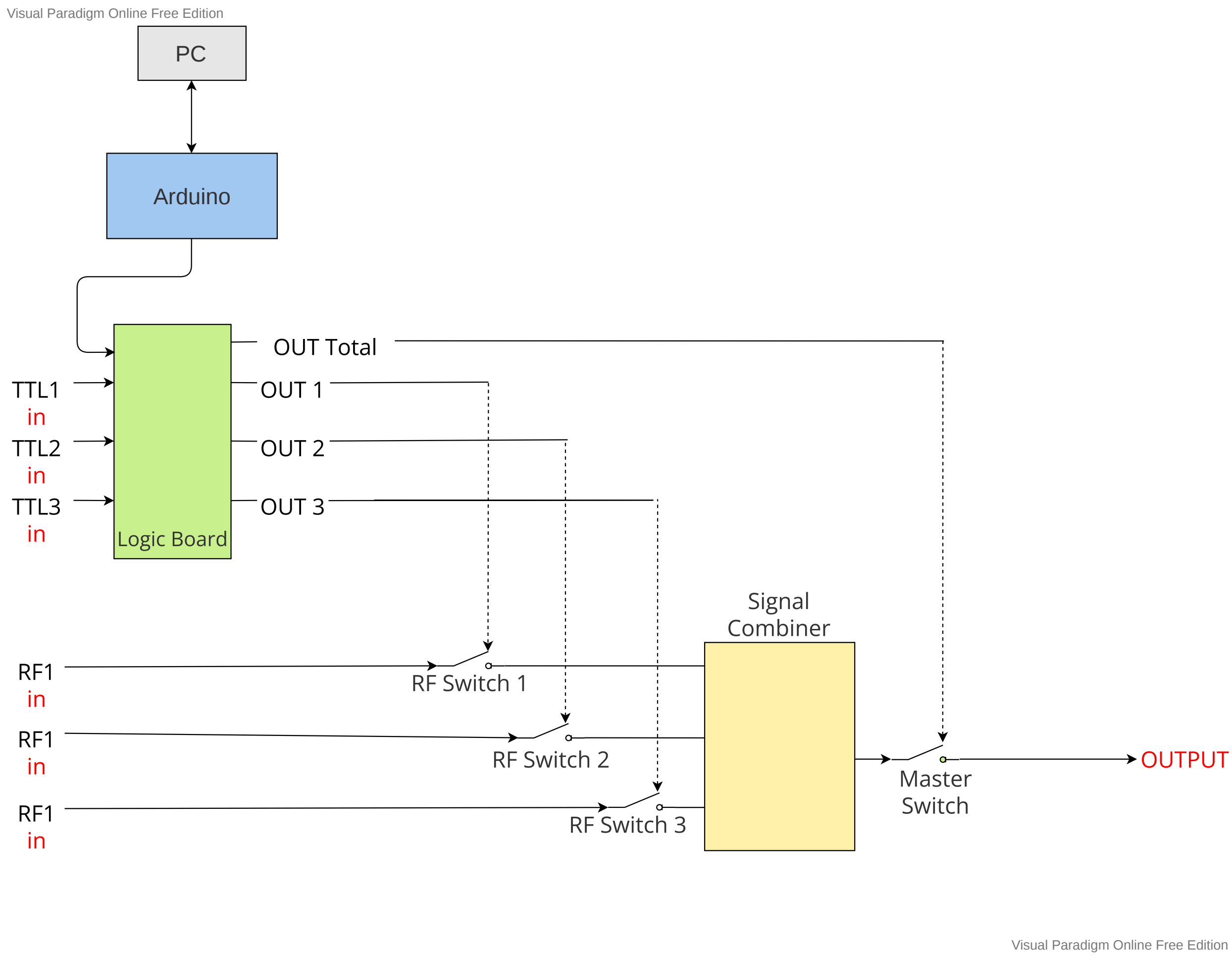

Figure 4: Schematic of the circuit of the box. All the elements in this box are powered via the power distribution board, not shown here to improve the readability of the schematic. See section 2.1.3 for detailed description of the outputs of the Logic Board.

2.1.3 Logic Circuit

The logic circuit determines which of the input RF signals will pass through to the output of the box. Each RF signal goes through a switch in the box that is opened by a TTL signal which is an output of the logic circuit. For example, if the 'Output TTL1' (in figure 5) is `True`, then the switch for RF1 will open and this RF1 signal will go to the output. The truth tables for the logic circuits are shown below. Each input/switch has its own logic circuit on the board according to table 1 and this determines the outputs `Output TTL 1, 2` and `3`. The `Output TTL total` is determined by the truth table 2. This last TTL signal goes to the 4^{th} switch in the box, and is `True` when any one of the three other outputs is `True`.

Figure 5 shows a labeled diagram of the PCB board of the logic circuit, and figure 6 shows an annotated schematic of the same circuit. Figure 7 shows the simplified circuit.

The data-sheets for the circuit elements used in this logic board can be found here:

- 3-way switches datasheet (Ref. [7])
- AND gates - model SN74LV21AD datasheet (Ref. [8])
- OR gates - model SN74AS32D datasheet(Ref.[9])
- NAND gates - model SN74AHC00D datasheet (Ref. [10])

The logic gates have a time delay of 5.8 - 7 ns when operated at 5V.

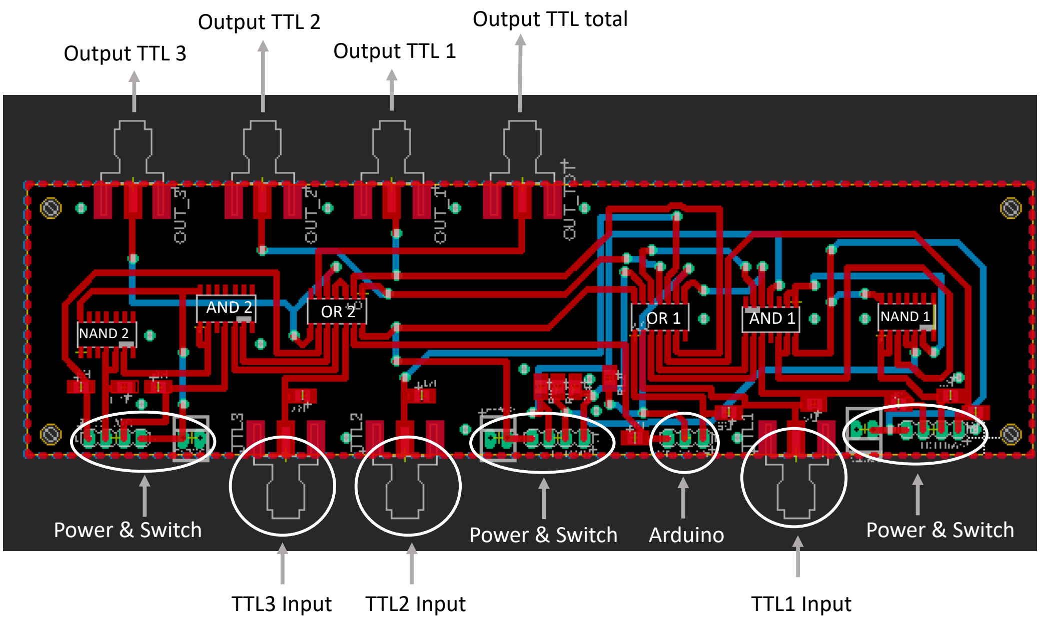

Figure 5: The TOP of the logic circuit board, annotated with the various inputs/outputs.

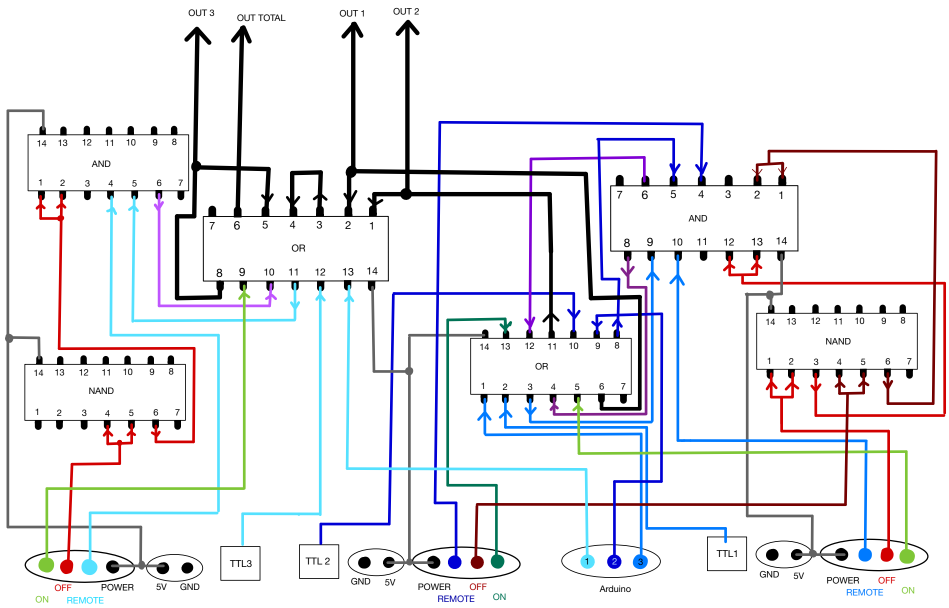

Figure 6: A colour coded schematic of the logic circuit. The resistors are not shown here for simplicity. All open pins are grounded.

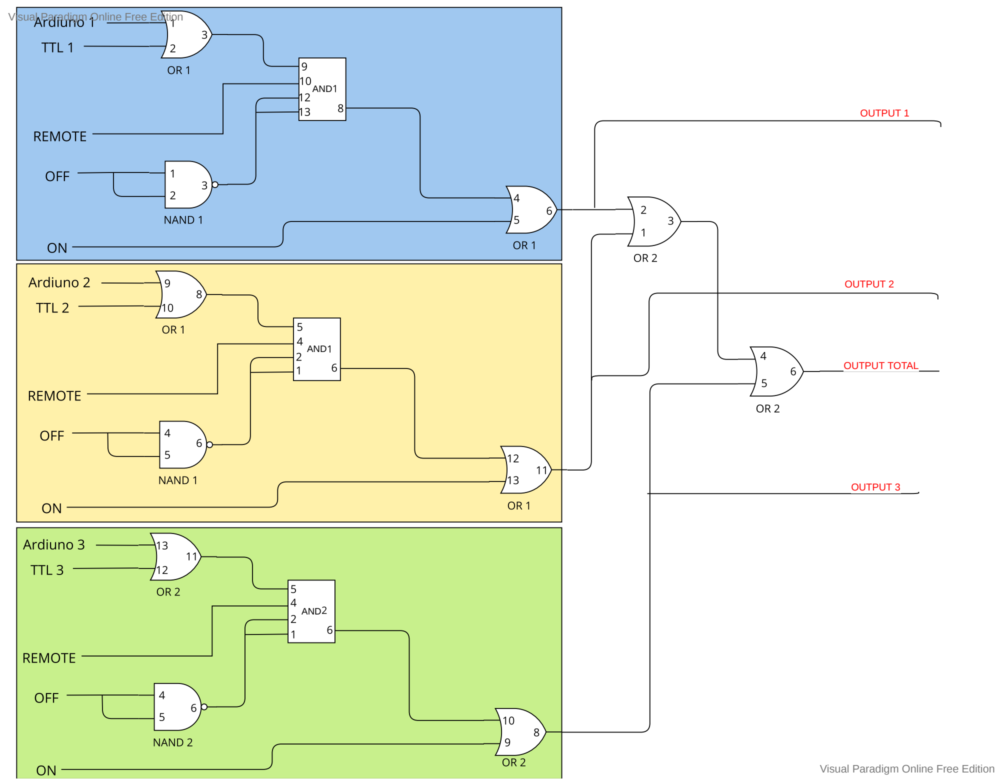

Figure 7: A simplified schematic of the logic board. All pins are labeled on the diagram.

Table 1: Truth table for the Logic Cicuit board, for one switch.

Switch			TTL Input	Arduino	Outputs
On	Remote	Off			
0	0	1	0 or 1	0 or 1	0
1	0	0	0 or 1	0 or 1	1
0	1	0	1	0	1
0	1	0	0	1	1
0	1	0	0	0	0
0	1	0	1	1	1

Table 2: Truth table for the Logic Cicuit board, for the TOTAL output.

Out_1	Out_2	Out_3	Out_{total}
1	0	0	1
1	1	0	1
1	1	1	1
0	1	1	1
0	0	1	1
1	0	1	1
0	1	0	1
1	1	1	1
0	0	0	0

2.1.4 Power Distribution Board & Power Supply

The power supply used in this box is a LASCAR PSU-206 (datasheet, Ref. [4]). It is wired to distribute -5V, +5V to the power distribution board which then transfers this power to the fast switches in the box. The power distribution board also delivers the 5V required to operate the ArduinoUNO and power the logic circuit. The power distribution board is designed as shown in figure 8.

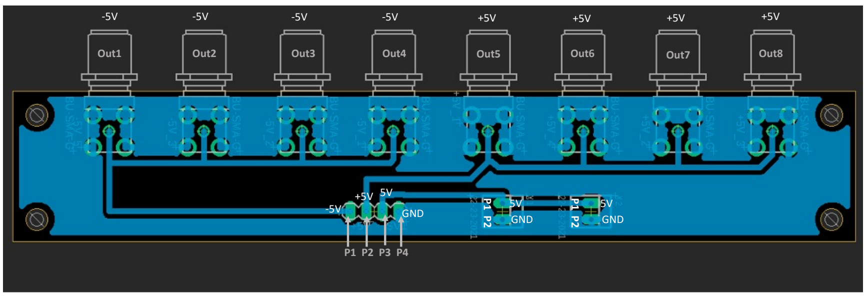

Figure 8: The power distribution board.

2.1.5 RF Switches & Combiners

The switches used in the box are ZASWA-2-50DRA+ (datasheet Ref. [5]).The RF combiners used are the ZFRSC-42+ (datasheet Ref. [6]).

2.2 Attenuation Tests & Timing Information

Here are the test results made to measure the attenuation and timing delays of the box.

2.2.1 Delay Timing of the Logic Circuit

The testing parameters used in this test are as follows:

- The arduino is turned off
- The TTL inputs are:
  - 1kHz square waves
  - $V_{pp} = 2.5V$
  - offset: 1.25V
  - Input cable: 10ns
- The Output cable: 1ns
- The trigger cable: 4ns

The resulsts of delay times of the circuit are shown in table 3. In this table, all the results are given with the cable delays subtracted.

Inputs		TTL Delay RISE time	TTL Delay FALL Time
SWITCH 1	OUT 1	15 ns	16.8 ns
SWITCH 1	OUT TOT	22.6 ns	23.6 ns
SWITCH 2	OUT 2	15 ns	17.6 ns
SWITCH 2	OUT TOT	21.2 ns	24.4 ns
SWITCH 3	OUT 3	15.2 ns	16.8 ns
SWITCH 3	OUT TOT	18.4 ns	21.0 ns

Table 3: Logic circuit delay time. Results have the cable delays subtracted.

2.2.2 Delay Timing of the Whole Box

The testing parameters used in this test are as follows:

- The arduino is turned off
- The TTL inputs are:

- 1kHz square waves
- $V_{pp} = 2.5V$
- offset: 1.25V
- Input cable: 4ns

- The RF inputs are:
  - Sine wave, 28 MHz
  - Amplitude: 0.00 dBm
  - Input cable: 4ns
- The Output cable: 5ns
- The trigger cable: 3ns
- Each switch used in the box has a 20ns delay.

The results are shown in table 4. All results have the cable delays subtracted.

Inputs	TTL			
	Delay RISE time[1]	Delay RISE Time[2]	Delay FALL Time[1]	Delay FALL Time[2]
INPUT 1	29.6 ns	57.4 ns	24.6 ns	34.2
INPUT 2	28.6 ns	56.6 ns	24.6 ns	31.8 ns
INPUT 3	27.8 ns	56.6 ns	23 ns	32.6 ns

Table 4: [1](trigger to first sign of change in RF signal) [2](trigger to first peak in RF signal). All the results have cable delays subtracted.

2.2.3 Attenuation Measurements

Here are the attenuation measurements of the box. All data was saved locally on the PC in the electronics lab, within the directory

`C:\ labdata \ 2022 \ June \ Testing Fast switch Box \ *.csv`

On the DFS, the data can be found at:

`dfs:\ Projects \ BASE2021 \ datalogger \ Testing Fast switch Box \ *.csv`

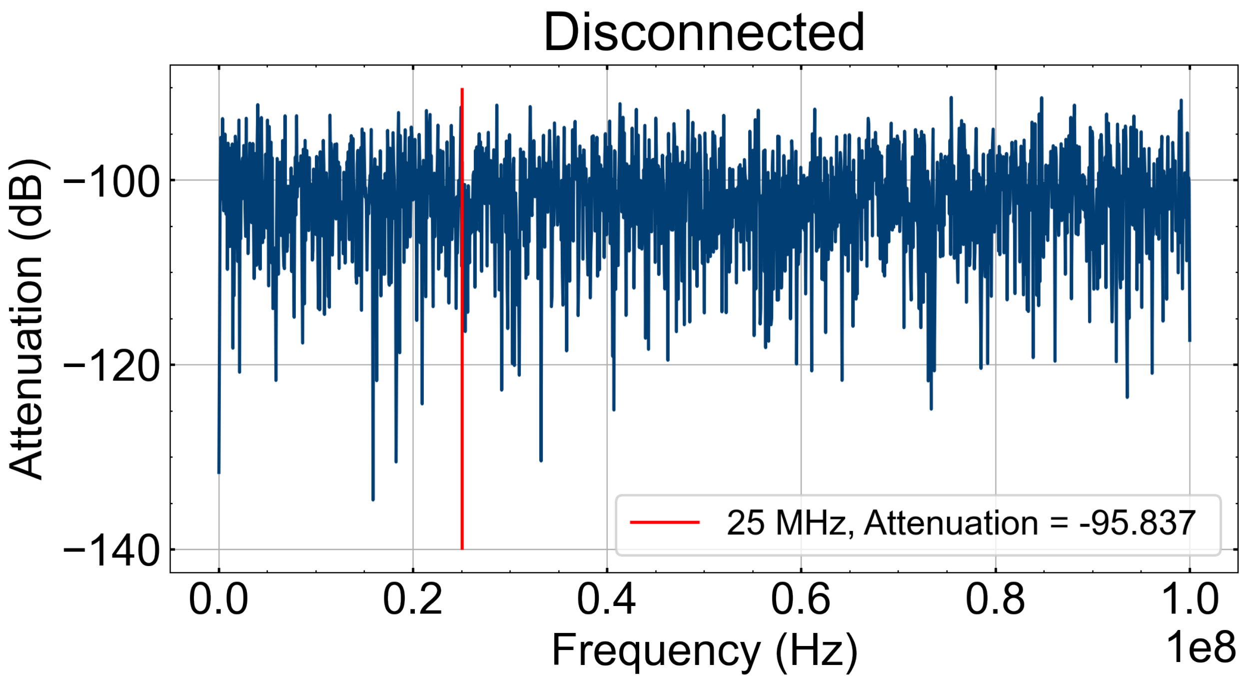

Figure 9: Attenuation with no inputs connected.

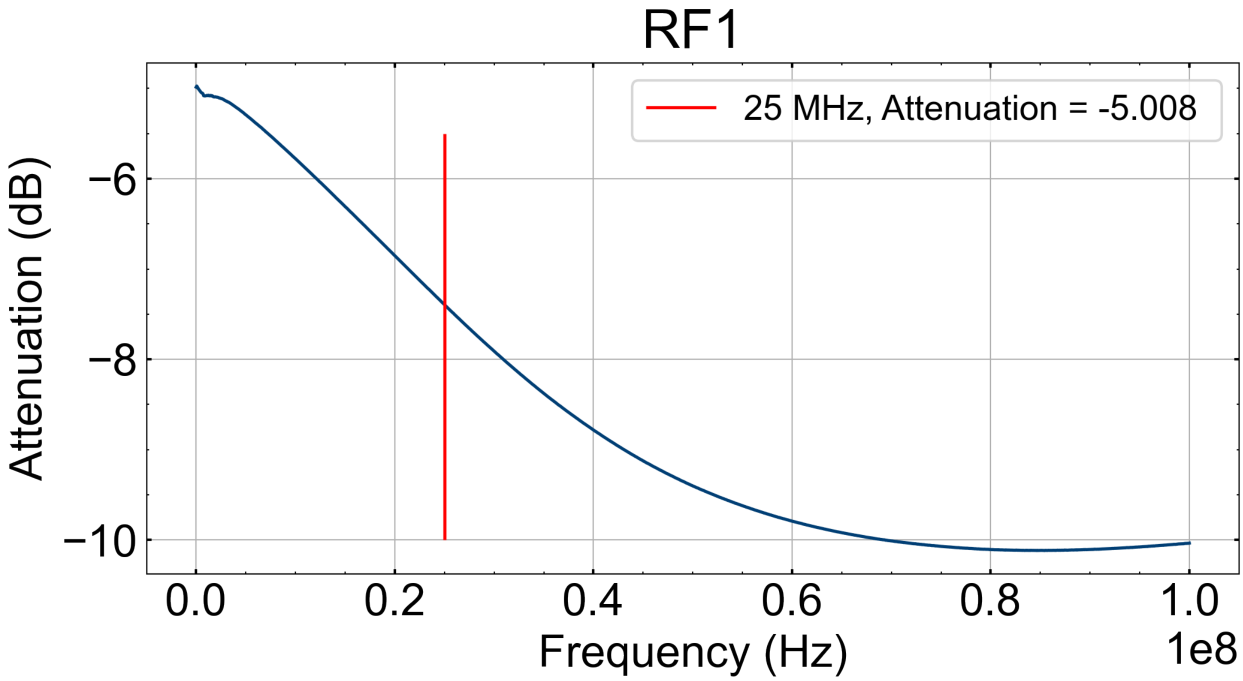

Figure 10: Attenuation with RF1 input connected.

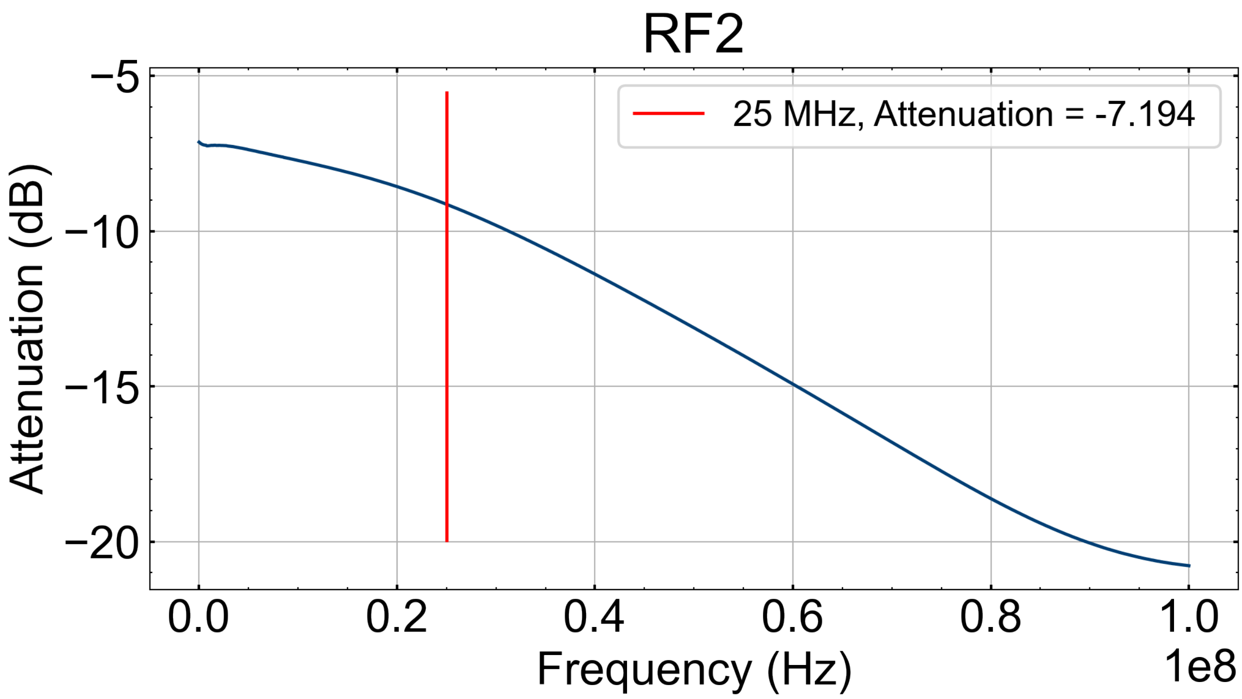

Figure 11: Attenuation with RF2 input connected.

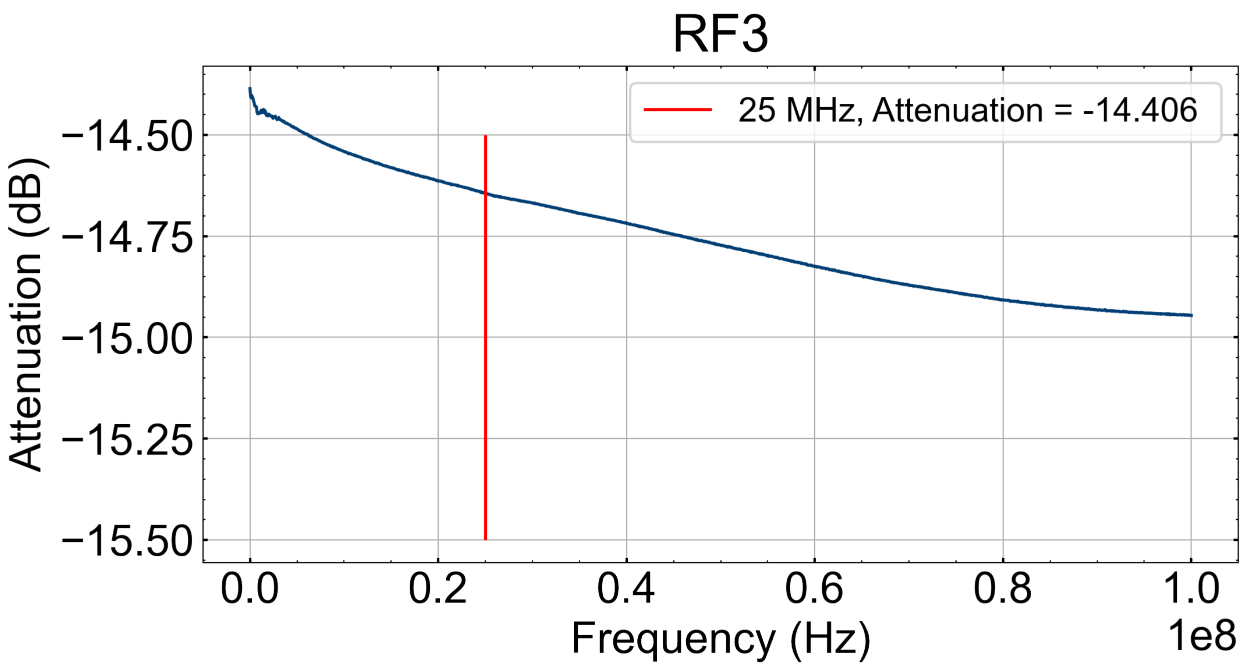

Figure 12: Attenuation with RF3 input connected.

3 Conclusion

The phase methods fast switch box was successfully implemented in the BASE experiment. The Arduino Uno code was included in the Labview interface, allowing easy remote operation of the box. This hardware was used successfully to operate the experiment and make preliminary phase sensitive measurements of the trapped particles. Looking forward, the BASE collaboration will be able to use this hardware for new phase methods with the goal of obtaining even more precise measurements.

References

[1] C. Smorra, K. Blaum, L. Bojtar *et al.*, "BASE – The Baryon Antibaryon Symmetry Experiment," *The European Physical Journal Special Topics*, vol. 224, no. 16, pp. 3055–3108, Nov. 2015.

[2] S. Ulmer, C. Smorra, A. Mooser *et al.*, "High-precision comparison of the antiproton-to-proton charge-to-mass ratio," *Nature*, vol. 524, no. 7564, pp. 196–199, Aug. 2015.

[3] M. J. Borchert, "Challenging the standard model by high precision comparisons of the fundamental properties of antiprotons and protons," Dec 2021.

[4] "Power supply datasheet." [Online]. Available: https://www.lascarelectronics.com/media/2780/psu-206.pdf

[5] "Rf switches datasheet." [Online]. Available: https://www.minicircuits.com/pdfs/ZASWA-2-50DRA+.pdf

[6] "Rf combiner datasheet." [Online]. Available: https://www.minicircuits.com/pdfs/ZFRSC-42+.pdf

[7] "3 way switch datasheet." [Online]. Available: https://docs.rs-online.com/f40f/A700000006783093.pdf

[8] "And gate datasheet." [Online]. Available: https://www.ti.com/lit/ds/symlink/sn74lv21a.pdf

[9] "Or gate datasheet." [Online]. Available: https://www.ti.com/lit/ds/symlink/sn74as32.pdf

[10] "Nand gate datasheet." [Online]. Available: https://www.ti.com/lit/ds/symlink/sn74ahc00.pdf